Finite-Difference Solution of the Poisson–Boltzmann Equation: Complete Elimination of Self-Energy

ZHONGXIANG ZHOU,* PHILIP PAYNE, and MAX VASQUEZ
Protein Design Labs, Inc., 2375 Garcia Avenue, Mountain View, California 94043

NAT KUHN and MICHAEL LEVITT
Department of Structural Biology, Stanford University School of Medicine, Stanford, California 94305-5400

Received 15 June 1995; accepted 1 November 1995

ABSTRACT

A new procedure to solve the Poisson–Boltzmann equation is proposed and shown to be efficient. The electrostatic potential due to the reaction field is calculated directly. Self-interactions among the charges are completely eliminated. Therefore, the reference calculation to cancel out the self-energy is not needed. © 1996 by John Wiley & Sons, Inc.

Introduction

The importance of electrostatic interactions in determining stability and functionality for biological systems is well documented in the literature.[1-7] However, accurate calculations of the electrostatic interactions continue to be a serious challenge to theoreticians, particularly when solvent is involved. Electrostatic interactions are long ranged and environment-dependent. Any effort to truncate the contributions beyond a preset distance or to substitute the heterogeneous environment with a homogeneous one has to be made cautiously.

For macromolecules in solution, the electrostatic interactions are extremely complicated. Nevertheless, a simple continuum model used by Kirkwood and Tanford proves to be very useful.[8,9] In this continuum model, the macromolecule is treated as a low dielectric cavity immersed in a high dielectric solvent. Other molecules in solution are seen by the macromolecule as a statistical average.[8,10] In the early days, macromolecules were modeled by spherical cavities with point charges distributed in them. With the advent of fast computers and efficient algorithms, the actual shape and charge distribution of macromolecules can be taken into

* Author to whom all correspondence should be sent. Present address: 10666 North Torrey Pines Road, Department of Molecular Biology (MB-19), The Scripps Research Institute, La Jolla, CA 92037.

CCC 0192-8651 / 96 / 111344-08

consideration in calculations of electrostatic interactions. In 1982, Warwicker and Watson used a finite-difference method to solve the Poisson equation for complicated systems.[11] Since then, powerful algorithms have been developed using the finite-difference method to solve the more realistic Poisson–Boltzmann equation, and have been applied successfully to many different systems.[12-20] Other methods, such as the boundary element method and the finite element method, have also been introduced and proven to be successful for solving the Poisson–Boltzmann equation.[21-27] There exists, though, a powerful alternative method for calculating the electrostatic interactions in solution. This is the Langevin dipoles method that uses a semimicroscopic description of the solvent instead of the continuum model.[28-30] In this article we will concentrate our attention exclusively on the finite-difference method.

The finite-difference method transforms the Poisson–Boltzmann equation into a set of difference equations by using an equally spaced grid.[12] All physical properties, such as charge distribution, ionic strength, and dielectric constant, are mapped onto the grid. The solution to this set of difference equations gives the electrostatic potential, together with a large number of other properties.[15,31] The successive overrelaxation method used by Nicholls and Honig[14] and the conjugate gradient method used by Davis and McCammon[16] are very efficient techniques for solving these difference equations.

The accuracy of the solution to the finite-difference method depends on the grid spacing: The smaller the spacing, the more accurate the solution. However, the self-energy of the charges in the system increases as the spacing decreases. Although the self-energy should, in principle, cancel out in actual calculations, the accuracy of the results will be substantially affected in practice when the self-energy becomes predominant. As pointed out by Bruccoleri,[32] the inverse relationship between the self-energy and the grid spacing results from the charging model used to map the charges onto the grid. Since a point charge is projected onto the eight nearest grid points, the interactions among these eight projected charges become stronger when the grid spacing becomes smaller. By uniformly distributing an atomic charge onto all grid points within the van der Waals radius of respective atoms, Bruccoleri was able to reduce the self-energy considerably.[32] Both the fractional charging model used by Klapper et al.[12] and the uniform charging model used by Bruccoleri[32] need a reference calculation to remove the self-energy. Luty et al.[33] have developed an efficient algorithm to calculate the self-energy for the fractional charging model. The algorithm can also be used in combination with the uniform changing model. Here we describe a procedure to eliminate the self-energy completely. This procedure leads to a direct computation of the potential due to the reaction field.

Methodology

We start with the continuum model. The interactions between solute atoms and atoms in solvent are described implicitly by the Poisson–Boltzmann equation[10]

$$\nabla \cdot \varepsilon \nabla\phi - \frac{\bar{\kappa}^2}{2}\left[\exp\left(\frac{e\phi}{kT}\right) - \exp\left(-\frac{e\phi}{kT}\right)\right] = -4\pi\rho$$

or

$$\nabla \cdot \varepsilon \nabla\phi\bar{\kappa}^2 \sinh\left[\frac{e\phi}{kT}\right] = -4\pi\rho \qquad (1)$$

where ε is the dielectric constant, ϕ is the electrostatic potential to be determined, ρ is the charge distribution within the low dielectric cavity, and $\bar{\kappa}^2 = 8\pi e^2 I/kT$ with I the ionic strength, e the unit charge, k the universal Boltzmann constant, and T the temperature. When the charges are continuously distributed, ρ is a smooth function. When the charges are point charges, ρ has singularities—it is a distribution which is a sum of three-dimensional delta functions for each source charge; for each such singularity in ρ, there is a corresponding singularity (pole) in the solution ϕ which blows up roughly as $1/r$. Of course, the singularities in ρ cannot be modeled well by a finite-difference equation. The source-free method we are going to develop here, on the other hand, uses the analytical (coulombic) solution to eliminate the singularities of ϕ. The modified differential equation (4) we need to solve has a solution which does not have poles and, hence, should be more accurately approximated by the finite-difference method.

When $\bar{\kappa}^2 = 0$ and ε = constant, eq. (1) reduces to the Poisson equation

$$\varepsilon_p \nabla^2\phi_c = -4\pi\rho \qquad (2)$$

Here we have used the cavity dielectric constant ε_p. The subscript c is used throughout this article

to differentiate the coulombic potential ϕ_c in eq. (2) from other approximations to ϕ. There is an analytical solution to eq. (2), given by the simple coulombic formula. We will denote this analytical solution by ϕ_c^A. The difference $\phi_\delta = \phi - \phi_c$ is the function we are looking for, which should have its singularities removed. Notice that when we combine eq. (2) with eq. (1) we obtain

$$\nabla \cdot \varepsilon \nabla\phi - \bar{\kappa}^2 \sinh\left[\frac{e\phi}{kT}\right] = \varepsilon_p \nabla^2\phi_c \qquad (3)$$

To obtain the differential equation for ϕ_δ, note that

$$\nabla \cdot \varepsilon \nabla\phi_\delta = \nabla \cdot \varepsilon \nabla\phi - \nabla \cdot (\varepsilon - \varepsilon_p)\nabla\phi_c - \nabla \cdot \varepsilon_p \nabla\phi_c$$

Applying eq. (3), we obtain

$$\nabla \cdot \varepsilon \nabla\phi_\delta = \bar{\kappa}^2 \sinh\left[\frac{e\phi}{kT}\right] - \nabla \cdot (\varepsilon - \varepsilon_p)\nabla\phi_c \quad (4)$$

Since ε is exactly equal to ε_p and $\kappa = 0$ near the charges, we completely eliminate the singularities from the right-hand side of eq. (4), and hence we can expect ϕ_δ to be a smooth function.

Equations (1)–(4) can all be solved by the finite-difference technique. The corresponding finite-difference equations are[†]

$$\phi_i^{(n)} = \frac{\sum_j \varepsilon_{ij}\phi_j^{(n-1)} + 4\pi q_i/h}{\sum_j \varepsilon_{ij} + \bar{\kappa}_i^2 h^2 N(\phi_i^{(n-1)})} \qquad (5)$$

$$\phi_{c,i}^{(n)} = \left(\sum_j \phi_{c,j}^{(n-1)} + \frac{4\pi q_i}{\varepsilon_p h}\right)\Big/ 6 \qquad (6)$$

$$\phi_i^{(n)} = \frac{\sum_j \varepsilon_{ij}\phi_j^{(n-1)} + 6\varepsilon_p\phi_{c,i}^{(n-1)} - \varepsilon_p\sum_j \phi_{c,j}^{(n-1)}}{\sum_j \varepsilon_{ij} + \bar{\kappa}_i^2 h^2 N(\phi_i^{(n-1)})} \qquad (7)$$

and

$$\phi_{\delta,i}^{(n)} = \frac{\sum_j \varepsilon_{ij}\phi_{\delta,j}^{(n-1)} + 6\varepsilon_p\phi_{c,i}^{(n-1)} + \sum_j(\varepsilon_{ij} - \varepsilon_p)\phi_{c,j}^{(n-1)}}{\sum_j \varepsilon_{ij} + \bar{\kappa}_i^2 h^2 N(\phi_i^{(n-1)})} - \phi_{c,i}^{(n-1)} \qquad (8)$$

Here, ϕ_i, $\phi_{c,i}$, $\phi_{\delta,i}$, and $\bar{\kappa}_i^2$ are ϕ, ϕ_c, ϕ_δ, and $\bar{\kappa}^2$ at a particular grid point i, respectively, q_i is the charge projected to the grid point i, ε_{ij} is the dielectric constant assigned to the midpoint of two nearest neighbor grid points i and j, h is the spacing of the grid, and $N(\phi_i^{(n-1)})$ corresponds to the nonlinear term in eq. (1) or (4). The summations in eqs. (5)–(8) are over the six nearest neighbors of i. The superscript (n) is used to denote the cycle in the self-consistent procedure of solving the equations. Notice that we will get the exact analytical coulombic potential ϕ_c^A from eq. (6) only when h goes to zero.

Because the ionic strength is zero and ε_{ij} equals ε_p within the low dielectric cavity, eq. (5) is identical to eq. (6) in this region. ϕ_c can be determined analytically, while the electrostatic potential within the cavity has to be solved self-consistently from eq. (5), or alternatively from eq. (7) coupled with eq. (6). Because all self-interactions of the charges are contained in ϕ_c alone, we can get the self-interaction-free electrostatic potential by simply taking away ϕ_c from ϕ, that is, by solving eq. (8). In so doing we replace ϕ_c in eqs. (7) and (8) with its analytical solution ϕ_c^A. Namely, instead of eqs. (7) and (8), we use

$$\phi_i^{(n)} = \frac{\sum_j \varepsilon_{ij}\phi_j^{(n-1)} + \varepsilon_p\left(6\phi_{c,i}^A - \sum_j \phi_{c,j}^A\right)}{\sum_j \varepsilon_{ij} + \bar{\kappa}_i^2 h^2 N(\phi_i^{(n-1)})} \qquad (9)$$

and

$$\phi_{\delta,i}^{(n)} = \frac{\sum_j \varepsilon_{ij}\phi_{\delta,j}^{(n-1)} + 6\varepsilon_p\phi_{c,i}^A + \sum_j(\varepsilon_{ij} - \varepsilon_p)\phi_{c,j}^A}{\sum_j \varepsilon_{ij} + \bar{\kappa}_i^2 h^2 N(\phi_i^{(n-1)})} - \phi_{c,i}^A \qquad (10)$$

Neither eq. (9) nor eq. (10) contains source charges explicitly; thus, they are source-free. The effect of charges is given by the analytical coulombic terms in the formulas. Equation (10) is superior to eq. (5) for four reasons. First, the source charges are absent from the equation, and so is the uncertainty associated with the grid charge assignment. Second, the reference calculation is not needed to obtain properties such as the solvation energy, because $\phi_{\delta,i} = 0$ for $\bar{\kappa}^2 = 0$ and ε = constant. Third, the potential due to the reaction field is calculated directly. The predominant self-interaction contributions near the point charges are eliminated; thus, the interaction energy of the system can be calculated more accurately. In fact, the self-energy is completely eliminated (see below). Finally, solvation energy can be calculated for actual higher-order multipoles. We do not have to model the higher-order multipoles by point charges. The simple coulombic potentials generated by any higher-order multipoles can be computed easily.

[†] See, for example, ref. 12 for derivation of eq. (5). All finite-difference equations can be derived similarly.

Implementation

As in any other finite-difference method, we place the low dielectric solute molecule at the center of a box that is large enough so that boundary conditions can be determined correctly. Here we only consider cubic boxes. An equally spaced grid is set up within the box. The dielectric and ionic strength parameters are mapped onto the grid as conventionally done.[12] The dielectric boundary is determined by the solvent accessible surface.[34]

The grid points are classified into four classes: (i) The box boundary points. The potential values at these points are kept constant; they are determined by the boundary value conditions. (ii) The low dielectric cavity region. In this region $\kappa = 0$ and ε is the low dielectric constant. (iii) The solvent region. In this region ε is the solvent dielectric constant. (iv) Dielectric boundary region. For regions (ii) and (iii), eq. (10) can be simplified. Particularly, for the cavity region $\phi_{\delta,i} = \Sigma\phi_{\delta,j}/6$.

We can consider two implementations of eq. (10). In the first instance, eq. (10) is used in both the solvent and the cavity regions. This is the source-free method. In the second instance, eq. (10) in the cavity region is combined with eq. (5) for the solvent region. This is the partial source-free method. In principle, the partial source-free method should allow more accurate calculation of the electrostatic potential in the solvent region. In practice, as evidenced by computed results, this is only true for grids much finer than atomic dimension. Meanwhile, we lose the simple solution of $\phi_{\delta,i} = 0$ for the reference calculation. Note that ϕ_c is larger in magnitude than ϕ_δ in the solvent region. These two equations are different in this region because of the fact that the exact simple coulombic potential is a solution to the difference equation (6) only as the grid spacing h approaches 0, as previously pointed out. Usually, we use a much coarser grid than that for the partial source-free model to be of any practical use. We will exclude it from further discussion.

Three types of boundary conditions are implemented at the box boundary points: zero boundary value, simple coulombic potential with the solvent dielectric constant, and the simple coulombic potential scaled by the Debye–Hückel rule.[31] We have used the simple coulombic potential with solvent dielectric constant at the box boundary. Also, we have employed the focusing technique to improve the boundary potential.[12] The difference equations are solved using the Gauss–Seidel algorithm. The successive overrelaxation technique is used to accelerate convergence.[14] The analytical coulombic potential ϕ_c^A can be calculated either directly or indirectly. Since our test cases involve only a small number of charges, we calculate ϕ_c^A directly.

Our program is written in C with dynamic memory allocation. For comparison purposes we have also implemented the charge assignment schemes developed by Klapper et al.[12] and by Bruccoleri.[32] We will denote these two implementations as fraction and uniform, respectively.

Results and Discussion

All results given in this section are from the linearized Poisson–Boltzmann equation, although our program is written for the solution of the full Poisson–Boltzmann equation. Our purpose here is to test our new source-free approach.

The simplest case to test is to put a spherical charge in a solvent. This is the well-known Born solvation process. We tested a unit charge of radius 2 Å in water. We chose the dielectric constants to be 78 for water and 1 for the charged sphere, for the results to be comparable with those reported by Bruccoleri.[32] The computed results are presented in Table I. The deviation of the solvation energy from the exact analytical solution decreases as the grid spacing h decreases; so does the dependence of the solvation energy on the charge location in the grid. The accuracy of the results from the source-free model is more or less the same as, or probably slightly better than, that from the other two models. However, the effect of the grid spacing is more important to the accuracy of the calculations than the charging model used. This conclusion generally holds true for all the systems we have tested.

The self-energy portion of the solvation energy is not reported in the table. The self-energy is completely eliminated in source-free calculations. This can be seen from eq. (10). When $\varepsilon_{ij} = \varepsilon$ and $\bar{\kappa}_i^2 = 0$, eq. (10) produces $\phi_{\delta,i} \equiv 0$. That is, the reference calculation with $\varepsilon = 1$ gives zero electrostatic energy. All electrostatic interactions in this case are self-interactions. The self-energy in the uniform charging model goes to the exact analytical self-energy of a spherical charge distribution as the grid spacing h goes to zero,[32] while the self-

TABLE I.
Deviation of Calculated Electrostatic Free Energy for a Spherical Ion in Water from the Exact Born Solvation Energy (−81.94 kcal/mol).[a]

Grid Spacing	Source-Free		Uniform		Fraction	
h (Å)	Deviation	Range	Deviation	Range	Deviation	Range
1.0	−5.90	14.68	−8.62	11.11	−6.91	15.13
0.5	−2.81	1.87	−3.47	2.09	−2.89	1.71
0.3333	−1.56	1.34	−1.87	1.18	−1.59	1.39
0.25	−1.06	0.46	−1.25	0.50	−1.09	0.45
0.2	−0.87	0.10	−1.00	0.12	−0.90	0.10
0.1667	−0.62	0.33	−0.75	0.32	−0.67	0.33

[a] The deviation is obtained by averaging over six sphere locations. The grid points used in this calculation are defined by a cubic lattice (ih, jh, kh), where i, j, and k are integers. The Born sphere was centered at the following six positions: $(0,0,0)$, $(h/3,0,0)$, $(h/3,h/3,0)$, $(h/3,h/3,h/3)$, $(h/2,h/2,h/2)$, and $(h/3.14,h/1.59,h/6.26)$. The deviation range over these six locations is also given. All energies in kilocalories per mole.

energy in the fraction charging model approaches infinity at this limit. To get *one* value of a solvation energy, we need to numerically solve the Poisson–Boltzmann equation only *once* in the source-free model, but *twice* in the other two models. As we pointed out earlier, the reference calculation in both the fractional and the uniform model can be simplified by the Luty–Davis–McCammon procedure.[33]

The next test we performed was a point charge in a spherical cavity. In this case the fraction and the uniform charging models are identical. Again, an analytical solution is available to this problem.[8] The solvation energies from all models along with the exact one are plotted in Figure 1(a) and the deviations from the exact solution are plotted in Figure 1(b). The radius of the cavity is chosen to be 10 Å. The finite-difference equations are set up within a 40^3 Å^3 cubic box. The cavity center coincides with the box center. The dielectric constants used are 2 for the cavity and 80 for the solvent. A unit point charge moves from 1 Å deep beneath the dielectric boundary toward the cavity center along the x direction. The solvation energy be-

TABLE II.
Percentage rms Error of Calculated Electrostatic Potential Derived from Different Charging Models in the Finite-Difference Poisson–Boltzmann Equation.[a]

	Source-Free				Uniform and Fraction			
r[b]	o	i	b	a	o	i	b	a
0.0	3.5	3.5	9.7	4.2	0.1	3.8	9.1	2.5
2.1	3.4	3.5	9.4	4.1	0.1	3.8	8.9	2.5
3.7	3.3	3.5	9.0	4.0	0.2	3.8	8.5	2.4
5.0	3.2	3.5	8.4	3.8	0.3	3.9	8.0	2.3
6.0	3.0	3.7	7.8	3.6	0.3	3.9	7.4	2.2
6.8	2.8	4.1	7.0	3.3	0.4	4.0	6.8	2.0
7.5	2.5	4.5	6.2	3.0	0.4	4.1	6.1	1.9
8.0	2.2	4.5	5.6	2.7	0.4	3.9	5.5	1.7
8.4	1.9	4.0	5.0	2.4	0.4	3.6	4.9	1.6
8.7	1.5	3.3	4.4	2.0	0.4	3.6	4.3	1.4
9.0	1.2	3.1	4.3	1.7	0.4	2.8	3.8	1.2

[a] The system is a unit point charge in a spherical low dielectric cavity. The analysis is done by classifying grid points into three categories: o, for grid points outside the dielectric cavity; i, for grid points inside the cavity; b, for grid points near the cavity/solvent boundary. a stands for all grid points.
[b] r is the distance between the point charge and the dielectric cavity center.

comes more negative as the charge approaches the dielectric boundary. The errors for all models also become larger. The source-free model gives similar, probably slightly better, solvation energies than the competing models. The charges near the dielectric boundary are more important to electrostatic interactions between solute and solvent than those charges buried deep inside the cavity. This is consistent with Tanford's observation that it is crucial that charges be distributed about 1 Å below the surface for a spherical protein model to generate the correct titration curves.[35]

Table II compares the computed electrostatic potentials with the exact solution. All models generate very good electrostatic potentials. Outside the low dielectric cavity the fraction or uniform charging model is marginally better than the source-free model. For the other two regions these three models give similar percentage root-mean-square (rms) errors in the electrostatic potentials. For the dielectric boundary region, the percentage rms error is much larger than those in the other two regions in all charging models.

Our third test examined the accuracy of the different models applied to a system of a dipole in a low dielectric cavity. All setups are the same as in Figure 1. Although we can directly do computations for actual dipoles, we will use point charge models for comparison purposes. All other models, including the exact solutions, used the point charge model. The dipole is composed of two unit point charges separated by 1 Å. Because dipoles have directions also, we examined two orientations of the dipole with respect to an x axis that extends from the cavity center to its surface. In the first case, the dipole is collinear with the x axis. In the second case, the dipole moment lies along a y axis and is perpendicular to the radial axis x. Figure 2(a) and (b) plot the distance dependence of the solvation energy and its deviation from the exact analytical solution (see ref. 8) for the x orientation. Figure 2(c) and (d) are the same plots for the y orientation. The solvation energy of a dipole embedded in a low dielectric cavity is much smaller. This can be seen from Figure 2. The results confirm the conclusions reached in the preceding examples. That is, the source-free model produces similar, probably slightly better, solvation energies, and the errors in computed solvation energies increase as the distance between the source charges and the dielectric boundary decreases. The solvation energies for dipoles more than 3 Å away from the dielectric boundary are all less that 1 kcal/mol. The solvation energy also

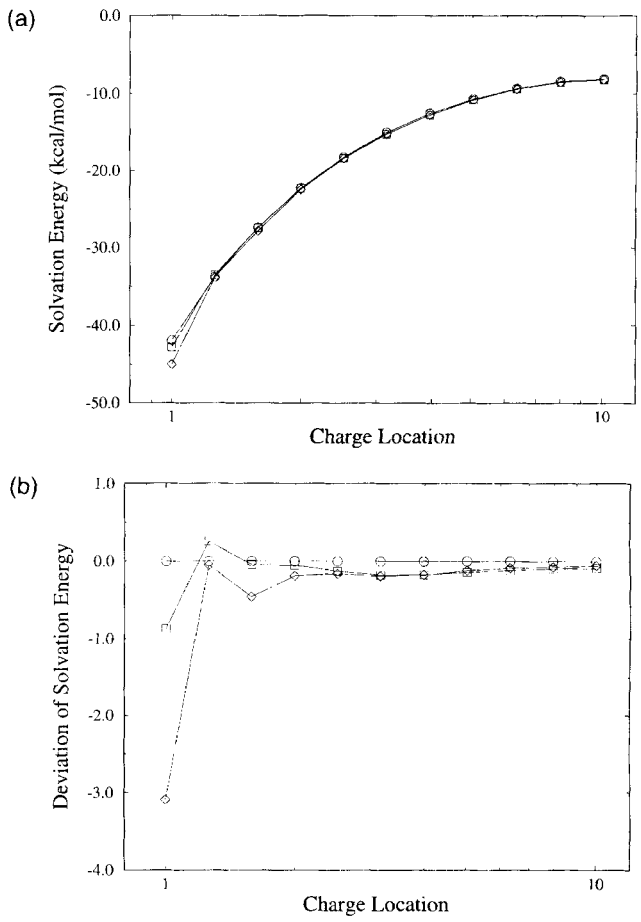

FIGURE 1. Solvation energy versus distance from the cavity surface for a point charge in a spherical cavity of radius 10.0 Å. The finite-difference Poisson–Boltzmann equation is solved on a 65 × 65 × 65 grid within a 40^3 Å^3 cube. A focusing technique is used to improve the boundary values at the grid box boundary. Symbols used: circle, exact result from Kirkwood formulas; square, calculated result from source-free model; diamond, calculated result from fraction or uniform charging model. (a) Solvation energy; (b) deviation from the exact solvation energy.

depends on the dipole orientation, as expected. The radial orientation of the dipole direction [Fig. 2(a) and (b)] induces a bigger reaction field than the other orientation [Fig. 2(c) and (d)]. Comparison of Figures 1 and 2 shows that contributions to the solvation energy are much larger from point charges than from dipoles. Therefore, the penalty for burying a dipole inside the interior of a protein is much smaller than that for burying a charged residue. This conforms to our intuition, experimental facts, and conclusions from other theoretical calculations.

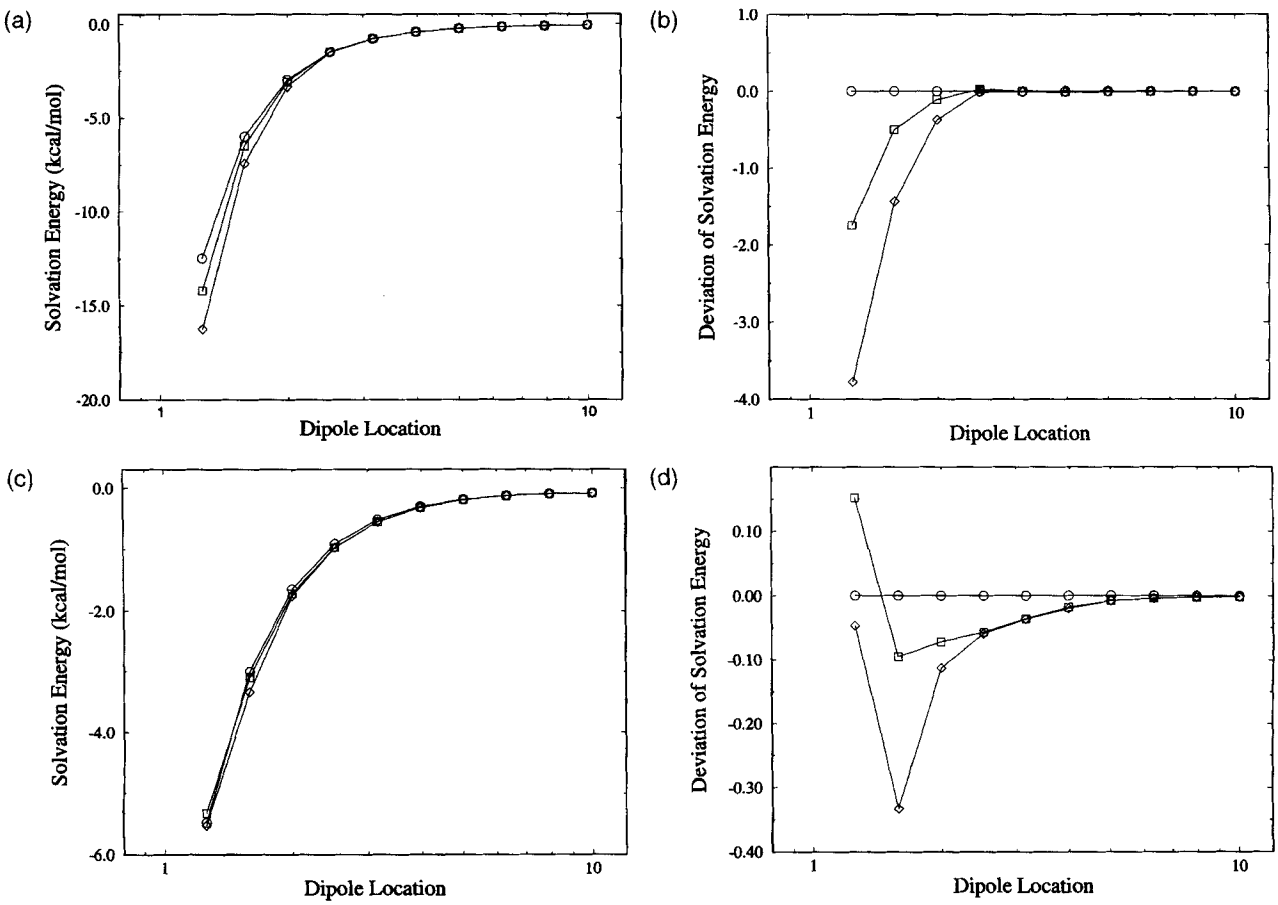

FIGURE 2. Solvation energy versus distance between the dipole center and the cavity surface for a dipole in a spherical cavity of radius 10.0 Å. The dipole is composed of two unit point charges of opposite sign separated by 1 Å. The finite-difference Poisson–Boltzmann equation is solved on a 65 × 65 × 65 grid within a 40^3 Å^3 cube. The focusing technique is used to improve the boundary values at the grid box boundary. Symbols used: circle, exact result from Kirkwood formulas; square, calculated result from source-free model; diamond, calculated result from fraction or uniform charging model. The dipole direction is the same as *x* direction and the spherical cavity is centered at the origin. (a) Solvation energy, Dipole center moves along *x* axis; (b) deviation from the exact solvation energy, dipole center moves along *x* axis; (c) solvation energy, dipole center moves along *y* axis; (d) deviation from the exact solvation energy, dipole center moves along *y* axis.

Before we conclude this section, it is worthwhile to point out that the advantage and/or disadvantage derived from the choice of a particular charging model is unlikely to have much significance, compared with errors that accrue from approximations used in the finite-difference equations.

Concluding Remarks

We have shown that the Poisson–Boltzmann equation can be solved directly to obtain the electrostatic potential excluding the self-interactions. This is done by separating the simple coulombic potential from the total potential. All self-interactions among the charges are included in the simple coulombic potential. Source charges are represented by the analytical coulombic potential. No source charges appear in the formulation. This eliminates both the singularities in the differential equation to be solved and the uncertainty associated with the charge projection scheme. The electrostatic free energy can be calculated more accurately.

By computing directly the potential due to the reaction field, we eliminated the reference calculation of getting the self-energy. Hence, we may achieve a slightly better accuracy of calculating the

electrostatic free energy. This is important, particularly for charges distributed near the dielectric boundary. These charges are important in determining, for example, the titration curves.[35]

Another important feature derived from the absence of source in our formulation is that we can solve the Poisson–Boltzmann equation for the actual higher-order multipoles while other charging models have to use point charges to model the multipoles. Since more advanced molecular mechanics potentials use dipole or distributed multipoles to describe electrostatics, our formulation should work better with these potentials than other charging models do (see, for example, ref. 36 and the references therein).

Acknowledgments

Helpful comments from Dr. Cary Queen and Dr. Shankar Kumar are gratefully acknowledged.

References

1. A. Brack and L. E. Orgel, *Nature*, **256**, 383 (1975).
2. M. F. Perutz, *Science*, **201**, 1187 (1978); *Protein Science*, **3**, 1629 (1994).
3. A. Warshel and S. T. Russel, *Quart. Rev. Biophys.* **17**, 283 (1984).
4. J. B. Matthew, *Ann. Rev. Biophys. Biophys. Chem.*, **14**, 387 (1985).
5. B. Honig, W. Hubbell, and R. Flewelling, *Ann. Rev. Biophys. Biophys. Chem.*, **15**, 163 (1986).
6. S. C. Harvey, *Proteins*, **5**, 78 (1989).
7. Y. Choo, I. Sánchez-García, and A. Klug, *Nature*, **372**, 642 (1994).
8. J. G. Kirkwood, *J. Chem. Phys.*, **2**, 351 (1934).
9. C. Tanford and J. G. Kirkwood, *J. Am. Chem. Soc.*, **79**, 5333 (1957).
10. See, for example, D. A. McQuarrie, *Statistical Mechanics*, Harper & Row, New York, 1976.
11. J. Warwicker and H. C. Watson, *J. Mol. Biol.*, **157**, 671 (1982).
12. I. Klapper, R. Hagstrom, R. Fine, K. Sharp, and B. Honig, *Proteins*, **1**, 47 (1986).
13. M. K. Gilson and B. Honig, *Nature*, **330**, 84 (1987).
14. A. Nicholls and B. Honig, *J. Comput. Chem.*, **12**, 435 (1991).
15. B. Honig, K. Sharp, and A.-S. Yang, *J. Phys. Chem.*, **97**, 1101 (1993).
16. M. E. Davis and J. A. McCammon, *J. Comput. Chem.*, **10**, 386 (1989); **12**, 909 (1991).
17. V. Mohan, M. E. Davis, J. A. McCammon, and B. M. Pettitt, *J. Phys. Chem.*, **96**, 6428 (1992).
18. D. Bashford and M. Karplus, *Biochemistry*, **29**, 10219 (1990).
19. A.-S. Yang and B. Honig, *J. Mol. Biol.*, **231**, 459 (1993).
20. J. Antosiewicz, J. A. McCammon, and M. K. Gilson, *J. Mol. Biol.*, **238**, 415 (1994).
21. R. J. Zauhar and R. S. Morgan, *J. Mol. Biol.*, **186**, 815 (1985); *J. Comp. Chem.*, **9**, 171 (1988); **11**, 603 (1990).
22. R. J. Zauhar, *J. Comput. Chem.*, **12**, 575 (1991).
23. A. A. Rashin, *Int. J. Quantum Chem., Quantum Biol. Symp.*, **15**, 103 (1988); *J. Phys. Chem.*, **94**, 1725 (1990).
24. H.-X. Zhou, *Biophys. J.*, **65**, 955 (1993).
25. B. J. Yoon and A. M. Lenhoff, *J. Comput. Chem.*, **11**, 1080 (1990); *J. Phys. Chem.*, **96**, 3130 (1992).
26. Y. N. Vorobjev, J. A. Grant, and H. A. Scheraga, *J. Am. Chem. Soc.*, **114**, 3189 (1992).
27. T. J. You and S. C. Harvey, *J. Comput. Chem.*, **14**, 484 (1993).
28. A. Warshel and M. Levitt, *J. Mol. Biol.*, **103**, 227 (1976).
29. A. Warshel, *Proc. Natl. Acad. Sci. USA*, **75**, 5250 (1978).
30. F. S. Lee, Z. T. Chu, and A. Warshel, *J. Comput. Chem.*, **14**, 161 (1993).
31. M. E. Davis and J. A. McCammon, *Chem. Rev.*, **90**, 509 (1990).
32. R. E. Bruccoleri, *J. Comput. Chem.*, **14**, 1417 (1993).
33. B. A. Luty, M. E. Davis, and J. A. McCammon, *J. Comput. Chem.*, **13**, 768 (1992).
34. B. Lee and F. M. Richards, *J. Mol. Biol.*, **55**, 379 (1971).
35. C. Tanford, *J. Am. Chem. Soc.*, **79**, 5340 (1957).
36. C. H. Faerman and S. L. Price, *J. Am. Chem. Soc.*, **112**, 4915 (1990).